ELSEVIER

Catalysis Today 52 (1999) 291–305

CATALYSIS TODAY

www.elsevier.com/locate/cattod

Oscillating reactions

I. Ferino*, E. Rombi

Dipartimento di Scienze Chimiche, Universita di Cagliari Via Ospedale, 72, 09124, Cagliari, Italy

Abstract

The features of oscillating reactions are reviewed. By means of familiar examples and simple kinetic models, the role of nonlinearity, multiplicity of steady states and stability against perturbations is outlined first. The Belousov–Zhabotinsky reaction is then briefly discussed as an example of homogeneous-phase chemical oscillator. The occurrence of oscillations and spatiotemporal patterns in heterogeneous catalysis is described, with particular attention to CO oxidation with O_2 on Pt surfaces as well as on supported catalysts in fixed-bed reactors.

Keywords: Oscillating reactions; Belouosov–Zhabotinsky; Heterogeneous catalysis; CO oxidation; Pt catalysts

1. General background

Oscillating reactions are a subset of phenomena in a widespread field dealing with the formation of structures ordered in space and/or time in physical and chemical systems; the science of chaos and turbulence also belong to this field. Such structures are maintained as long as matter and/or energy flow through the system assuring the highest rate of entropy production and are hence called dissipative structures. The underlying thermodynamic considerations are beyond the scope of the present contribution; the interested reader can address to [1].

The establishing of an oscillating behaviour can be traced back to some general features of the system, whatever its nature. These can be conveniently outlined here by considering a homogeneous chemical reaction operated in a CSTR, i.e. a system rather familiar to both chemists and chemical engineers. Indicating the chemical reaction by the general notation $\Sigma_j \alpha_j A_j = 0$ (A_j is the generic species and α_j its stoichiometric coefficient, positive for products and negative for reactants), the behaviour of this system is governed by the mass and energy balance equations:

$$\tau(\mathrm{d}\xi/\mathrm{d}t) = -\xi + \tau r(\xi, T), \quad (1)$$

$$\tau(\mathrm{d}T/\mathrm{d}t) = (T - T_0) + \tau J r(\xi, T), \quad (2)$$

where ξ is the reaction extent, τ the space–time, $r(\xi,T)$ the reaction rate, T_0 the inlet temperature, $J(=\Delta H/C_P)$, the ratio between the enthalpy of reaction and the overall heat capacity (per unit volume). The solutions of Eqs. (1) and (2) can be represented as trajectories in the ξ versus T plane (the phase-plane plot), which for $t \to \infty$ can approach either a single fixed point (Fig. 1) or a set of fixed points (Fig. 2). These points individuate the steady states. Whatever its initial composition and temperature, the system in Fig. 1 evolves towards the single steady state, which can be regarded as an attractor for the system. (Note that this situation does not correspond to the achievement of the chemical

*Corresponding author. Tel.: +39-70-6758602; fax: +39-70-6758605
E-mail address: ferino@vaxca1.unica.it (I. Ferino)

0920-5861/99/$ – see front matter
PII: S0920-5861(99)00083-8

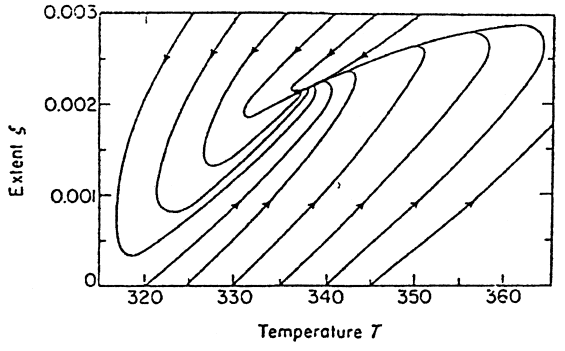

Fig. 1. Phase portrait for a single steady state (from Ref. [4]).

equilibrium; the latter is the attractor for the reaction operated in a batch reactor, i.e. a closed system). The system in Fig. 2 is attracted by point A (a low temperature steady state with poor conversion) whenever the initial conditions fall in the region at the left of the dashed EBD curve (called separatrix); starting from anywhere at the right of EBD leads instead to point C

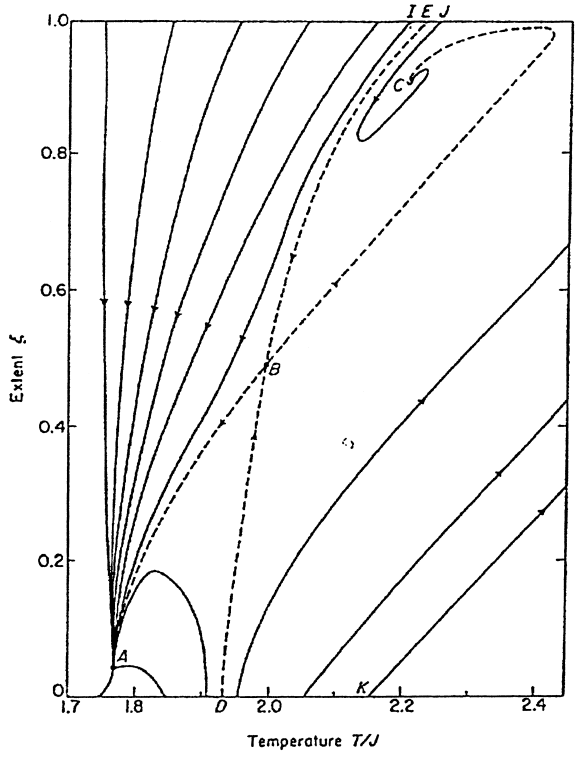

Fig. 2. Phase portrait for three steady states (from Ref. [4]).

(a high temperature-high conversion steady state). Both A and C are stable steady states in the sense that small fluctuations of T and ξ are bound to die out, as will be shown later on. Point B represents a third, unstable steady state; though it seems possible to approach it by following the dashed path, this cannot happen in practice because the slightest, unavoidable perturbation causes the system to follow a trajectory which ultimately takes it away from the neighbourhood of B and leads it either towards A or C.

An intuitive approach to the stability of the steady states can be easily developed for an irreversible, first-order reaction A→B (details can be found in many textbooks, see for instance [4,5]). When the steady state condition is attained the first member in both Eqs. (1) and (2) becomes zero; Eq. (1) gives then the expression for c_A:

$$c_A = c_{AO}/(1 + \tau k(T)) \quad (3)$$

which can be introduced in Eq. (2) to give:

$$(T - T_0) + k(T - T_{CO}) = J\tau k(T)/(1 + \tau k(T)), \quad (4)$$

where T_{CO} is the inlet temperature of the external coolant stream and k is a constant depending on the constructive characteristics the cooling system. The left-hand side in Eq. (4) is proportional to the rate of heat removal from the system (U_r), the right one to the rate of heat generation in the system (U_g), i.e. the steady state is attained when the heat is generated in and removed from the system at the same rate. Solving Eq. (4) gives the steady-state temperature, which in a plot of U_r and U_g versus T is individuated by the abscissa of the intersection point between the U_r and U_g curves. The former is a straight line, whose intercept and slope depend on the feed temperature and flow rate, respectively; U_g is a s-shaped curve, which, for a given reaction, varies with the feed flow rate [5]. Accordingly, one or more intersections are possible, as sketched in Fig. 3, i.e. there are circumstances in which more than one steady state is compatible with a given set of feed conditions. (Note that it is the nonlinear shape of the heat generation curve which makes possible the occurrence of multiple steady states). The stability of the steady states A and C against temperature fluctuations is automatically assured: in both cases a casual shift of T to the right of its stationary value moves the U_r line above U_g, i.e. the heat is removed faster than is generated and T is

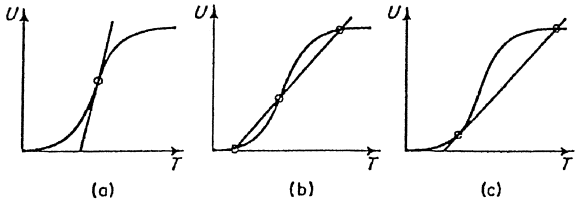

Fig. 3. Possible intersections of the heat generation curve with the heat removal line.

forced to decrease; a casual shift of T to the left makes U_r to lie below U_g, which forces T to increase back. The steady state B is unstable: a casual increase of T above its steady value increases the heat generation rate more than its removal, which in turn results in a further increase of T until the stable steady state C is attained; the opposite occurs for a casual decrease of T and the system leaves B to reach the stable state A.

The effect of changing the feed temperature and flow rate is presented in Figs. 4 and 5, respectively, together with the resulting hysteresis of the steady states. In practice the system can shift from a lower steady state with extinct reaction to an upper stable state with ignited reaction (and vice versa) as a consequence of slight variations of the feed temperature and flow rate (the control parameters). This is the so-called parametric sensitivity of the system [2,3], well-known to chemical engineers for the related potential hazards. The occurrence of such a bistability is often presented under the form of a bifurcation diagram (Fig. 6).

For a deeper inspection of the system behaviour, the effect of small perturbations occurring around the steady states should be carefully considered. The general procedure for a system with two state variables can be found in [6], where all the permissible behaviour types are discussed. Briefly, for the present case the deviations of ξ and T from the stationary values are given by the following set of differential equations [4]:

$$\tau(\mathrm{d}x/\mathrm{d}t) = -Lx + (N/J)y, \tag{5}$$

$$\tau(\mathrm{d}x/\mathrm{d}t) = J(1-L)x - (M-N)y, \tag{6}$$

where $x=\xi-\xi_S$; $y=T-T_S$; $L=1-\tau(\partial r/\partial\xi)$; $M=1+(\mathrm{d}Q/\mathrm{d}T)$; $N=J\tau(\partial r/\partial T)$; $Q=k\,(T-T_{CO})$. The solutions of Eqs. (5) and (6) are of the type:

$$x = \mathrm{A}_1 \exp(m_1 t/\tau) + \mathrm{A}_2 \exp(m_2 t/\tau), \tag{7}$$

$$y = \mathrm{B}_1 \exp(m_1 t/\tau) + \mathrm{B}_2 \exp(m_2 t/\tau), \tag{8}$$

where m/τ are the so-called Lyapunov exponents and m_1 and m_2 are the roots of the dispersion equation,

$$m^2 + (L+M-N)m + (LM-N) = 0. \tag{9}$$

Real and complex roots are possible, which results in quite different solutions for Eqs. (7) and (8). Accordingly, the fate of the perturbation can be quite different, as shown in Figs. 7 and 8. Perturbations can die out (which means a stable steady state) or grow exponentially, undergo sustained oscillation and even oscillate with exponentially increasing amplitude (the steady state is unstable). It can be shown that stability

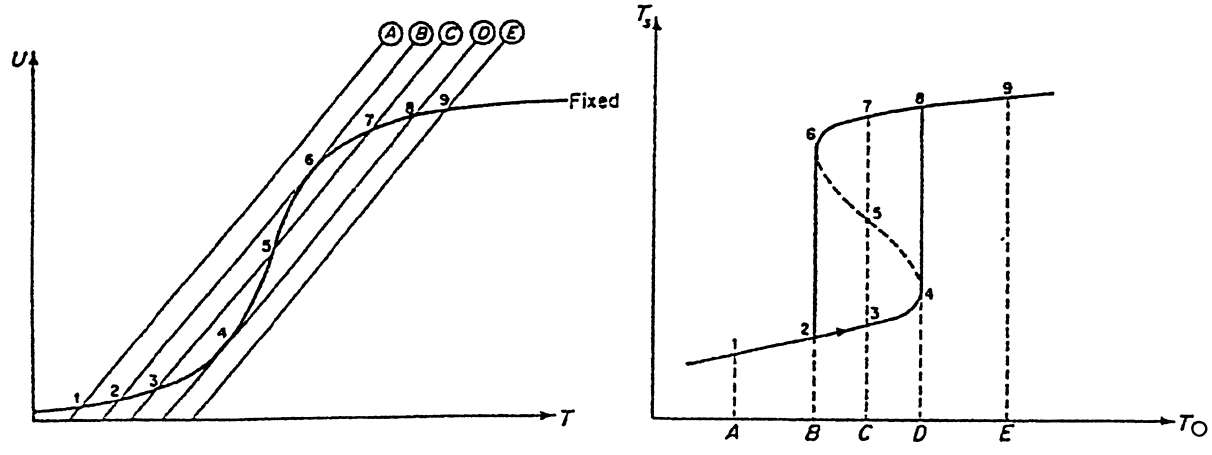

Fig. 4. The effect of changing the feed temperature (from Ref. [4]).

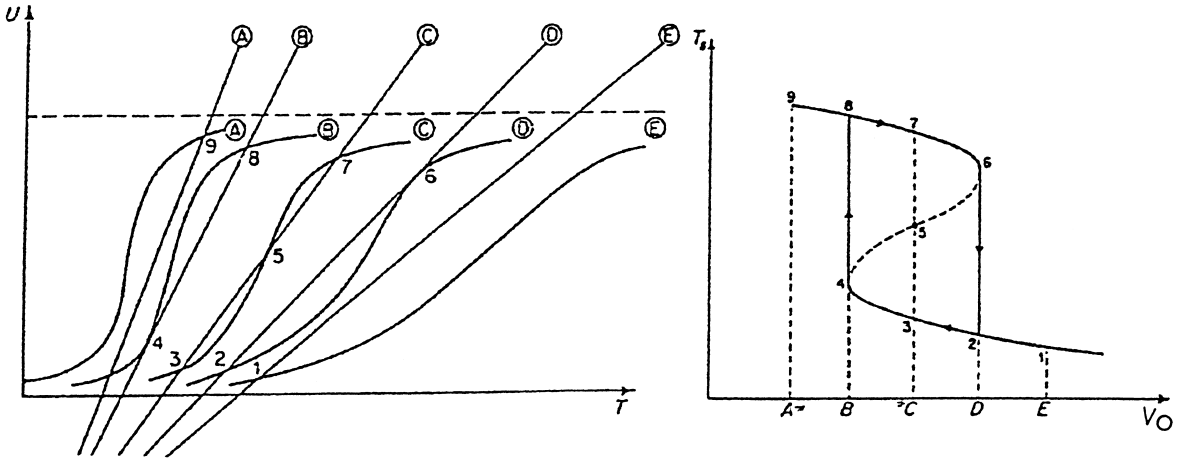

Fig. 5. The effect of changing the flow rate (from Ref. [4]).

occurs whenever $L+M>N$ and, simultaneously, $LM>N$. Thus, the behaviour of the system depicted in Fig. 2 is such because the parameter values assure the stability conditions in A and C but not in B. A and C in Fig. 2 are examples of stable nodes [6], where perturbations die out as in Fig. 7. B in Fig. 2 is a saddle point [6], where any perturbation grows as in Fig. 8 and causes the system to decay to A or C. In principle, one could try to change M (for instance through a better control of the coolant stream) in order to make stable the state B. In doing so, however, it could happen that the former behaviour is completely lost and the phase portrait becomes like that in Fig. 9. That is, in a particular range of the parameter values, the perturbations in the vicinity of the unstable state B are amplified (as for curve C in Fig. 8) and pervade the whole system causing the disappearing of the stable steady states. Instead, a cyclic attractor around an unstable focus [6] appears (Fig. 9): whatever the starting conditions, the system is now bound to reach a state where it will oscillate indefinitely, i.e. the temperature and the reaction extent will change periodically with time (this is explicitly shown in Fig. 10).

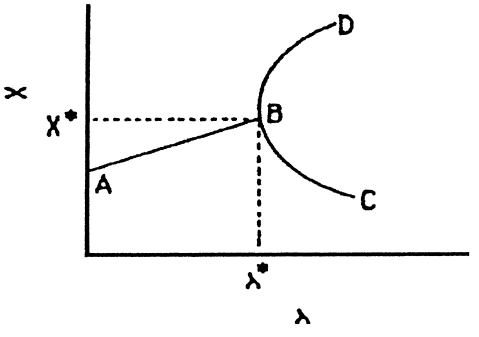

Fig. 6. Bifurcation diagram.

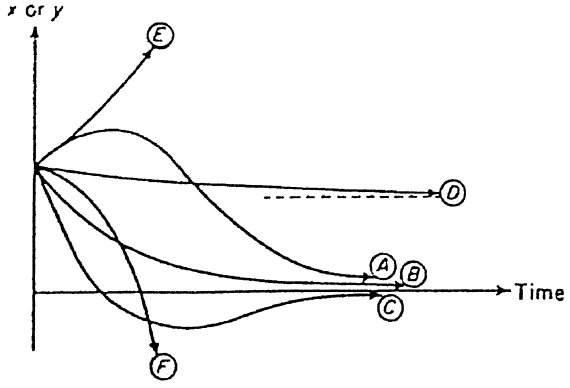

Fig. 7. Types of solutions corresponding to real roots (from Ref. [4]).

The key points of the above discussion can be summarised as follows:

1. the system is far from equilibrium;
2. the equations describing the involved phenomena are nonlinear;
3. multiple steady states are hence possible;
4. their stability against fluctuations is not always assured and

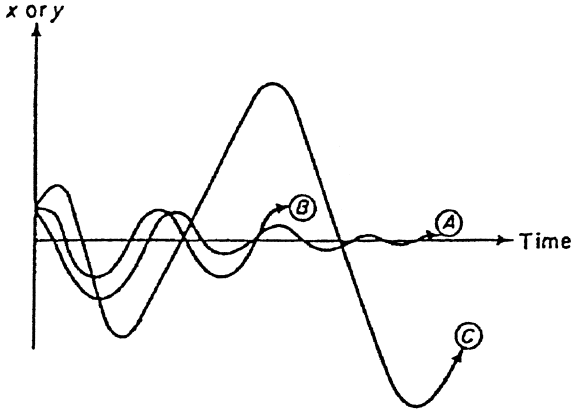

Fig. 8. Types of solutions corresponding to complex roots (from Ref. [4]).

5. within a critical range of the control parameters sustained oscillations set in.

Apparently, the oscillating behaviour can be traced back to the occurrence of (1) and (2) conditions; it should be stressed however that these are necessary but not sufficient conditions.

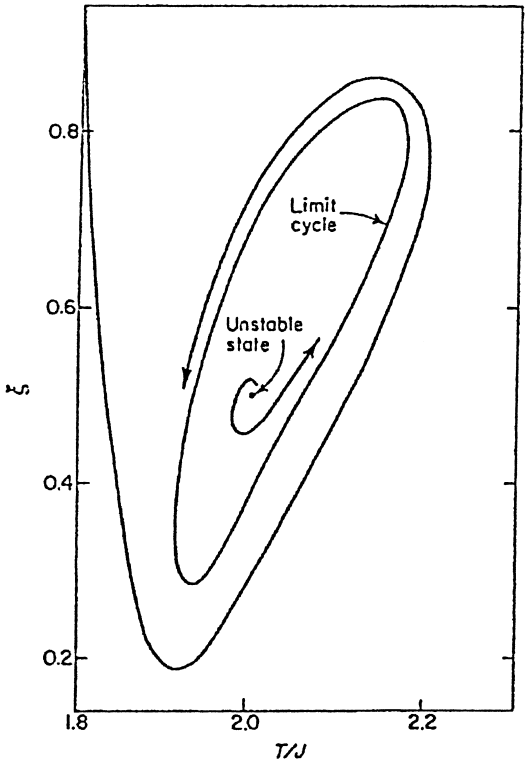

Fig. 9. The phase plane with a limit cycle (from Ref. [4]).

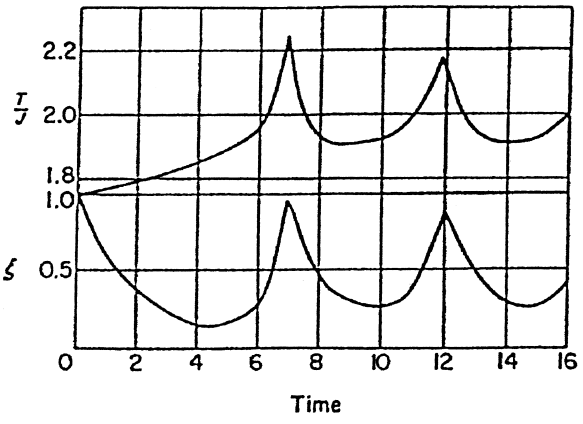

Fig. 10. Limit cycle behaviour as a function of time (from Ref. [4]).

Consider now the following reaction model [7]:

$$\begin{aligned} &A \rightarrow X2 \\ &X + Y \rightarrow 3X \\ &B + X \rightarrow Y + D \\ &X \rightarrow E \end{aligned} \qquad \text{(I)}$$

The concentrations of A and B are kept constant (e.g. by pumping). Each step is assumed irreversible and the system is thus far from equilibrium. The autocatalytic step involving a thermolecular reaction is a convenient way for introducing nonlinearity. The necessary conditions for oscillating behaviour are thus obeyed (cf. the preceding section). The concentration of the intermediates X and Y change with time as follows (the kinetic constants are assumed 1 for simplicity):

$$dc_X/dt = c_A + c_X^2 c_Y - c_B c_X - c_X, \qquad (10)$$

$$dc_Y/dt = c_B c_X - c_X^2 c_Y. \qquad (11)$$

The system has one steady state at $c_{XS}=c_A$ and $c_{YS}=c_B/c_A$. Stability analysis allows to take into account perturbations through the equations:

$$c_X = c_{XS} + x\exp(\omega t), \qquad (12)$$

$$c_Y = c_{YS} + y\exp(\omega t), \qquad (13)$$

where ω are the roots of the dispersion equation

$$\omega^2 + (c_A - c_B + 1)\omega + c_A^2 = 0. \qquad (14)$$

The real part of these roots is positive for $c_B > 1 + c_A^2$. In this domain of concentrations the perturbations are amplified (cf. Fig. 8, C curve) and

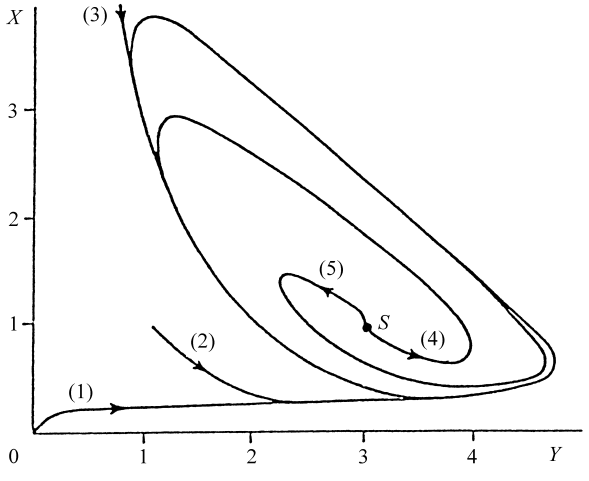

Fig. 11. Limit cycle for the reaction scheme (I).

the system leaves the steady state (which now behaves as an unstable focus) to approach a limit cycle (Fig. 11), where a sustained oscillation of X and Y concentrations persists indefinitely. The development of such a limit cycle from a stable steady state by sweeping a control parameter across a critical value can be represented by a bifurcation (the so-called Hopf bifurcation) as in Fig. 12.

So far, the model (called Brussellator) has considered the effect of perturbations which are homogeneous in space. It should be noted however that coupling between reaction and diffusion rates may occur in the autocatalytic steps, if the perturbation is space-dependent. To take this into account Eqs. (12) and (13) are modified by adding to each, respectively, the diffusional terms $D_X\,(\partial^2 c_X/\partial r^2)$ and $D_Y(\partial^2 c_Y/\partial r^2)$, where r is a space co-ordinate and D_X and D_Y the diffusional coefficients [7]. The analysis of the possible solutions of the corresponding dispersion equation reveals the permissible behaviours. Without entering into details, if two real roots are obtained, an instability point exists for a critical value of B concentration corresponding to an opposite sign of the

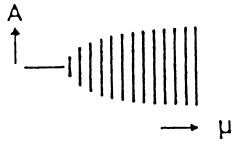

Fig. 12. Hopf bifurcation. The vertical lines denote oscillation amplitudes of a signal A.

roots; beyond this point (which individuates a so-called Turing bifurcation), if D_X and D_Y are different enough, the system approaches a new stable steady state which is space-dependent, i.e. the concentrations of both X and Y are constant in time but vary in space. If both the roots are complex conjugate, transition to instability sets in when their real part is zero and leads to a limit cycle whenever the real part becomes positive; this cycle is now space-dependent, i.e. the state variables now oscillate with respect to both time and space. It is intuitive that a local increase of the concentration of an autocatalytic species X, caused by a fluctuation, is further increased in that region because of the autocatalysis; this makes X to diffuse towards an adjacent region of the system, where, due to the autocatalysis, X production is enhanced and so on. As a result a concentration wave forms and travels through the system.

The Brussellator is one among the several model reactions [6] which have been proposed since the pioneering work of Lotka [8,9]. They confirm that the periodic behaviour may arise in systems far from equilibrium which are governed by nonlinear equations and provide a sound basis for interpreting the experimentally observed oscillating behaviour of real chemical systems. (It is worthy of note that the Lotka model, which fails to represent a real chemical system because of stoichiometric and thermodynamic constraints [6], has been successfully applied to describe the oscillations of the predator and prey populations in an ecological system [10]).

2. Homogeneous-phase chemical oscillators

The best-known example of a chemical oscillator is the liquid-phase Belousov–Zhabotinsky reaction (B–Z) [11], which has a long time been the main focus of the studies in the field [12]. In its classical version, the BZ reaction is the bromuration and oxidation of an organic substrate (usually malonic acid or its derivatives) by bromate ions in acidic solution, catalysed by either metal ions or their complexes. The oscillating behaviour can be spectacularly revealed when the catalyst has a different colour in its two different oxidation states. This is the case of Ce^{4+} (yellow) and Ce^{3+} (colourless); the oscillation of Ce^{4+} concentration (which can be traced quantitatively either

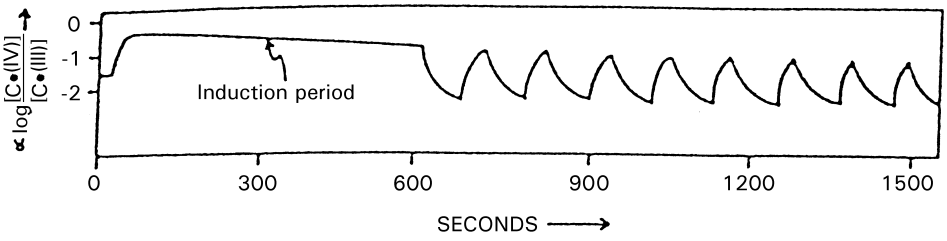

Fig. 13. Typical BZ oscillations (from Ref. [15]).

by spectrofotometry or potentiometry, Fig. 13), causes a periodic, macroscopic colour change in the solution. The overall stoichiometry is [13]:

$$2BrO^{3-} + 3CH_2(COOH)_2 + 2H^+ \rightarrow 2BrCH(COOH)_2 + 4H_2O + 3CO_2 \quad (15)$$

The first proposed mechanism (called FKN, after the authors' names), involving 21 intermediate species and 18 elementary steps [13], has been further detailed [14] with the individuation of 80 elementary steps (the so-called GTF mechanism). One of the key points is the following (overall) autocatalytic process in $HBrO_2$:

$$BrO_3^- + HBrO_2 + 2Ce^{3+} + 3H^+ \leftrightarrow 2HBrO_2 + 2Ce^{4+} + H_2O \quad (16)$$

In spite of its complexity, the mechanism has been modelled through a relatively simple scheme, called Oregonator [15,16]:

$$\begin{array}{lll} \text{process A} & A + Y \rightarrow X + P & \text{(a)} \\ & X + Y \rightarrow 2P & \text{(b)} \\ \text{process B} & A + X \rightarrow 2X + Z & \text{(c)} \\ & 2X \rightarrow A + P & \text{(d)} \\ \text{process C} & Z \rightarrow fY & \text{(e)} \end{array} \quad \text{(II)}$$

Two main sets of reactions exist in the real system, which are reduced in the model to processes A and B (the latter is a set of radical reactions while the former is nonradical). The control of the system switches back and forth between process A and B because these are coupled by a third set of reactions, called C. Identification of the real chemical species in the model is as follows: A=BrO^{3-}; P=HOBr; X=$HBrO_2$; Y=Br^-; Z=$2Ce^{4+}$; the concentration of A (the stoichiometrically significant species) is assumed constant (this is true in a CSTR; it is a reasonable assumption in a batch reactor because each oscillatory cycle consumes only a very small fraction of BrO^{3-}); HOBr is considered to be a dead-end product; the concentrations of H^+ and Ce^{3+} are assumed constant and taken into the kinetic constants. In a batch reactor, the system exists in a sort of bistable condition, represented by A and B processes: consumption of Y (=Br^-) through process A leads to process B; after a delay while Z (=Ce^{4+}) and P (=HOBr) accumulate, process C poisons process B by the production of Y from products of process B. Through process C reduction of Ce^{4+} back to Ce^{3+} also occurs, allowing to reinitialise process C for the next oscillation. True bistability occurs when the BZ reaction is operated in a CSTR [16]. Switching back and forth between control by process A and control by process B is shown in Fig. 14.

The dynamic approach requires to write the kinetic equations for the three variable species X, Y and Z (flow terms will not appear, unless a CSTR is used) and to solve them for the steady state conditions (better-said pseudo-steady state conditions for the batch case). The system has one such a state, which can behave as either a stable focus or an unstable node, according to the control parameters (f and the rate constant of step (e)) and independent of the initial conditions. In the former case the steady state is approached through damped oscillations, in the latter the system approaches a limit cycle. Because of the number of composition variables (three) the limit cycle should appear in a three-dimensional phase space; its projections in various planes can be conveniently presented. It should be stressed however that the border separating the regions in which the system is attracted by the steady state or the limit cycle is not always neat [16]. Within a range of parameter values the steady state and the limit cycle can exist simultaneously, both being only locally stable and separated by an infinitesimally unstable cycle (this situation is called a subcritical Hopf bifurcation). Infinitesimal

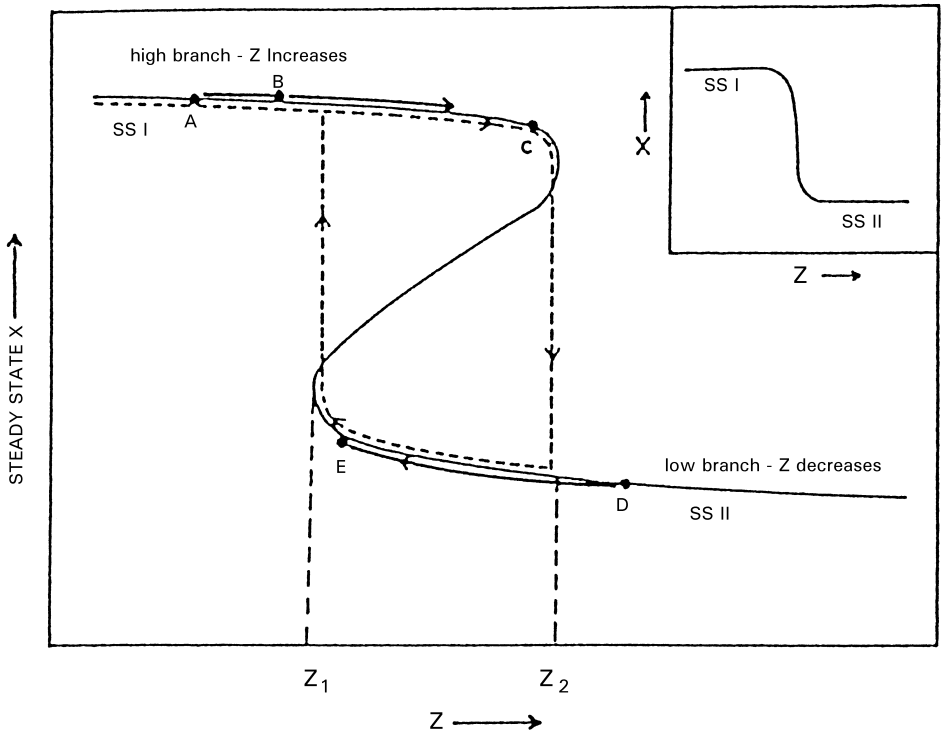

Fig. 14. Plot for steady state X versus Z, for scheme (II) (from Ref. [15]).

perturbations, always present in a real system, cause the system to evolve to either the locally stable steady state or the locally stable limit cycle; the evolution of the system depends on the direction of the perturbation, i.e. whether the perturbed trajectory finds itself in the attractive region of the steady state or the limit cycle.

A variety of interesting (and spectacular) spatial patterns originated by the coupling of diffusion and chemical rates can be observed in the BZ system (see for instance [17]). Many other liquid-phase oscillating reactions have been reported (see the literature cited in [16] and, for biochemical systems, in [18,19]).

3. Oscillatory reactions in heterogeneous catalysis

The possible occurrence of oscillations and spatio-temporal patterns in heterogeneous catalytic systems has received much attention since the early 1970s [20–22]. Most of the studies have focused on the CO oxidation with O_2, which is catalysed by group VIII noble metals and some oxides. Oscillatory behaviour has been observed also in the oxidation of H_2, NH_3, hydrocarbons, methanol and ethanol by O_2, the reduction of NO by CO, H_2 and NH_3, the Fisher–Tropsch reaction, the hydrogenation of ethylene and nitrobenzene, the decomposition of methylamine. A survey of these reactions, including information about the nature and type of catalysts, as well as the experimental techniques, can be found in [20–22]. Such a widespread occurrence and the lack of an universally acknowledged mechanism justifies, at least in part, the interest for the oscillatory catalytic reactions. It is believed that the analysis of these phenomena can reveal useful information about the factors influencing the catalyst performance and the potential hazards and benefits related to operating reactors in unstable regimes.

Oscillations in heterogeneous catalysis are very complex phenomena. At least in principle, it is possible to describe the system by formulating a set of differential equations representing the change with time of the surface concentrations (c_i, the state vari-

ables) of the species involved in the overall reaction. These rate equations can be derived by the elementary reaction steps and have the general form:

$$dc_i/dt = F_i(c_j, p_k), \quad (17)$$

c_j being all the state variables and p_k the external parameters (T, partial pressures...). Their solution gives the trajectories in the phase-space, which for $t \rightarrow \infty$ may approach fixed points (corresponding to steady states), limit cycles (periodic oscillation of the state variables and hence of the reaction rate) or even more complex behaviour (mixed-mode oscillations or chaos). Eq. (17) assumes spatial uniformity of the state variables. It should be noted however that spatial nonuniformities are unavoidable (even for a single crystal surface with a 30 mm^2 area) and different local oscillators exist; their contributions would average out and no macroscopic rate oscillation would be observed unless a synchronisation mechanism were operating. The more complex the macroscopic system, the more stringent the synchronisation requirements. Consider a packed-bed reactor, where the CO/O_2 reaction is operated over a supported Pt catalyst. Oscillations may occur on the Pt(1 0 0) face of the Pt crystallites, but these will be observed at the macroscopic level only if the reaction on the (1 0 0) facet oscillates in synchronisation, other (1 0 0) facets synchronise in the crystallite, other crystallites in the pellet couple to the first crystallite, and finally all the pellets in a layer of the bed oscillate in synchrony. If lack of synchronisation occurs on one of these levels, different oscillations superimpose and their effects will cancel; this might result in the increase of the noise level of the measured conversion. If independent synchronisation occurs over several regions of the system, the latter might behave in a chaotic way because of incomplete coupling. Synchronisation can be achieved:

1. via heat transfer through either the catalyst, the support or the gas phase;
2. through partial pressure variations in the gas phase, caused by an oscillation of the rate of consumption on the surface;
3. by surface diffusion of adsorbed species or phase transition of the surface structure.

Coupling of the different parts of the system will be transmitted through a generalised diffusion coefficient and Eq. (17) is modified as follows:

$$\partial c_i/\partial t = F_i(c_j, p_k) + D_i(\partial^2 c_i/\partial r^2), \quad (18)$$

where D_i is the generalised diffusion coefficient and r a space co-ordinate. If the time-scale of the associated transport process is comparable or slower than the period of the temporal oscillation, macroscopic wave propagation phenomena are to be expected. It should be stressed that each reaction has its own oscillating mechanism, generalisation being possible only to some extent (for instance by grouping of model mechanisms in classes). In the following the case of the catalytic CO oxidation is shortly presented (see [20–22] for a thorough discussion).

The reaction occurs on Pt catalysts and is by far the most extensively investigated system. An example of the different kinds of oscillations which can arise in CO/O_2 reaction is shown in Fig. 15 [23]. The development of rate oscillations upon variation of CO partial pressure at various temperatures is shown in the bifurcation diagram of Fig. 16 [24]. At low p_{CO} the reaction rate is first-order with respect to CO, but it becomes of minus first-order with respect to CO at high p_{CO}. The rate oscillations are observed within the

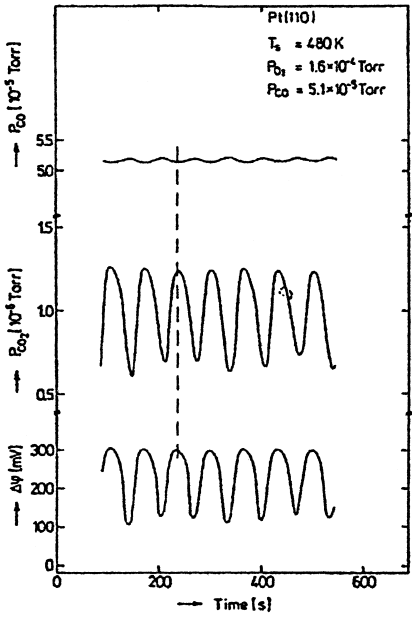

Fig. 15. Oscillations for the CO/O_2 reaction on Pt(1 1 0) (from Ref. [22]).

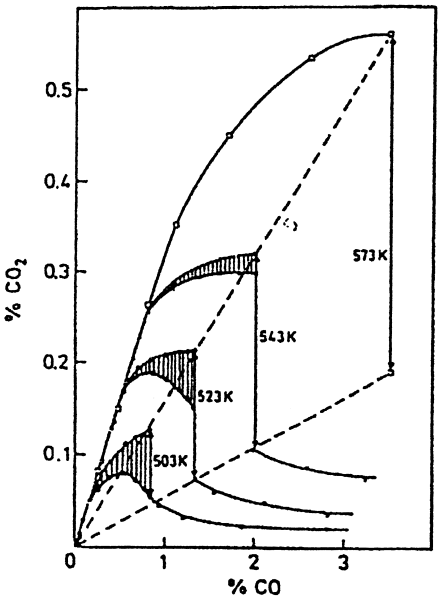

Fig. 16. Bifurcation diagram for CO/O_2 reaction on Pt/Al_2O_3–SiO_2 at P=atmospheric (from Ref. [23]).

intermediate range of p_{CO}, in the vicinity of the rate maximum; their amplitude increases with CO concentration and decreases (and finally disappears) with temperature.

The reaction mechanism for CO oxidation is based on the following sequence of elementary steps:

$$\begin{aligned} &CO + * \leftrightarrow CO_{ad} && (a)\\ &O_2 + 2* \rightarrow 2O_{ad} && (b)\\ &CO_{ad} + O_{ad} \rightarrow CO_2 + 2* && (c) \end{aligned} \qquad \text{(III)}$$

The asterisk indicates an adsorption site, which is however different for the two adsorbates. CO adsorption is characterised by the formation of densely packed layers, which, beyond a critical coverage, inhibits the dissociative oxygen adsorption; on the contrary, oxygen adsorption occurs through formation of an open layer, which allows CO adsorption to take place even at full oxygen coverage. The initial sticking coefficient for the oxygen adsorption depends on the structure of the Pt surface, while the sticking coefficient for CO adsorption is close to unity whatever the structure of the surface.

The reaction rate is:

$$R = dc_{CO_2}/dt = k_4\Theta_0\Theta_{CO} \qquad (19)$$

and the coverages Θ_{CO} and Θ_0 are given by:

$$d\Theta_{CO}/dt = k_1 p_{CO}[1 - (\Theta_{CO}/\Theta_{CO}^{sat})^r] - k_2\Theta_{CO} - k_4\Theta_{CO}\Theta_0, \qquad (20)$$

$$d\Theta_0/dt = k_3 p_{O_2}[1 - (\Theta_{CO}/\Theta_{CO}^{sat} - \Theta_0/\Theta_0^{sat})]^2 - k_4\Theta_{CO}\Theta_0, \qquad (21)$$

k_1 and k_2 are the forward and reverse rate constants of step (a); k_3 and k_4 the rate constants of step (b) and (c), respectively. k_1 and k_3 are given by the initial sticking coefficients. CO adsorption depends on coverage through the value of the exponent r (whose value is between 3 and 4 for a 110 surface); oxygen adsorption requires two neighbour empty sites, which can be occupied by either O or CO.

In the low p_{CO} region the surface is covered by an oxygen layer but still accessible for CO molecules, which are adsorbed whenever they strike the surface and then react with the adjacent O atoms; accordingly, the rate is zero-order with respect to O_2, being limited by CO adsorption. The latter increases as p_{CO} is increased but beyond a critical value inhibits O_2 adsorption; accordingly the rate reaches a maximum and then decreases, becoming limited by O_2 adsorption. Two states of the surface are thus possible, where either O or CO coverage predominates, i.e. the system exhibits bistability and a clockwise hysteresis may be expected upon variation of p_{CO}. Though the hysteresis effects can be related to the nonlinearity of Eqs. (20) and (21), the latter in no way are able to predict the rate oscillations experimentally observed in the transition range between high and low reactivity. An additional mechanistic step is needed to explain the oscillatory behaviour. Consider the three clean Pt surfaces shown in Fig. 17. The atomic arrangement for the topmost layer of Pt(1 1 1) is the same as for the corresponding bulk plane, i.e. of the 1x1 type. For the Pt(1 0 0) and Pt(1 1 0) clean surfaces the topmost layer differs from the underlying bulk plane, showing a hexagonal arrangement of the surface atoms in the former case and a 1×2 arrangement (so-called missing row type) in the latter.

The key observation is that oscillations are reported to occur upon reacting CO and O_2 over both (1 0 0) and (1 1 0) surfaces, whereas over the stable (1 1 1) surface merely bistability can set in (which can be described within the frame of the above mechanism)

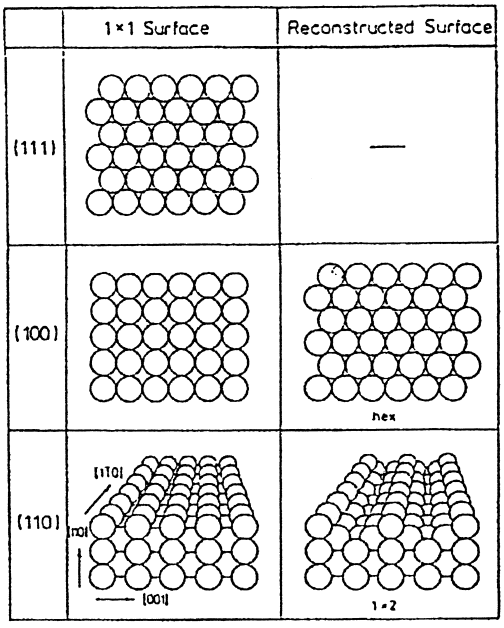

Fig. 17. Models of nonreconstructed bulk termination (left) and reconstructed surface (right) for Pt.

but no oscillations occur under any conditions. The microscopic process governing the macroscopic kinetics in the case of (1 0 0) and (1 1 0) surfaces is related to CO-induced phase transitions which alter the geometry of the topmost layer of Pt atoms. CO can adsorb on a clean (1 0 0) hexagonal surface, and beyond a critical total coverage, it induces a transition from the hexagonal to the 1×1 arrangement of the topmost layer of Pt atoms. The driving force for this hexagonal $\rightarrow$ 1×1 phase transition is the gain in adsorption energy (37 kcal/mol for the 1×1 phase versus 27 kcal/mol for the hexagonal) which overcompensates the energy necessary for altering the geometry of the clean surface; this process has no noticeable activation energy. This transformation is reversible: upon depletion of the local CO coverage on the 1×1 surface below a critical value (due for instance to thermal desorption or reaction), the surface reverts back to the hexagonal phase (the process has an activation energy of ca. 25 kcal/mol). It must be added that on a clean (1 0 0) hexagonal surface oxygen adsorption is almost negligible, the sticking coefficient being $\approx10^{-4}$–10^{-3}, whereas it can occur on the 1×1 phase, where the sticking coefficient is $\approx$0.3–0.4. On this basis the oscillating behaviour (which is observed when the surface is largely covered by CO and the oxygen adsorption is limiting the reaction rate) can be explained as follows:

1. the surface phase is mostly of 1×1 type;
2. O_2 adsorption occurs only at surface defects (inevitably present) with a high sticking coefficient;
3. the adsorbed O atoms react with adjacent CO molecules;
4. CO_2 immediately desorbs;
5. two empty sites are now present on the 1×1 phase and the oxygen uptake autocatalytically increases and so does the rate;
6. as CO rapidly reacts, its coverage on the 1×1 phase drops below the critical value that renders the 1×1 phase metastable and the surface transforms into the hexagonal phase;
7. the oxygen uptake drops because of the too small sticking coefficient and the reaction is quenched;
8. as CO coverage increases, the hexagonal $\rightarrow$ 1×1 transformation occurs and the oscillation begins anew.

The mechanism is basically the same for the (1 1 0) surface: in this case switching between the 1×2 and 1×1 phases (controlled by critical CO coverages) occurs; (these phases now differ in the sticking coefficient for the oxygen adsorption only by a factor of 2). The mechanism has been experimentally confirmed; it has been modelled on the basis of the coupled set of differential equations (20) and (21) by formulating a new equation to include the CO-induced structural transformation of the surface and by modifying Eq. (20) in order to take into account the different oxygen sticking coefficients on the 1×1 and 1×2 patches (see [20,22] for details).

The kinetic oscillations are usually rather regular on Pt(1 1 0). For a single-crystal experiment the heat released by the reaction is negligible compared to the heat continuously fed to the crystal to keep it isotherm and heat transport effects do not play any role. Variation of the reaction rate during the oscillations causes variation of the partial pressure of CO (ca. 1%, cf. Fig. 15). Under the low pressure conditions of the experiment ($<10^{-4}$ Torr) such a variation propagates so fast that any other part of the system is reached within a time that is shorter than the period of the oscillations by several orders of magnitude. A positive feedback effect is associated to p_{CO} variation:

as the reaction rate increases p_{CO} decreases, which in turn enhances the reaction rate; oscillations occur under conditions for which oxygen adsorption is rate-limiting, which is enhanced by lowering of the CO coverage (pressure). This positive effect may also trigger less reactive regions. Spatial differences of the surface concentrations will be of minor influence and the whole system can oscillate essentially in phase.

Though quite regular, the oscillations in the CO/O_2–Pt (1 1 0) system show some interesting features, which can be revealed by operating the reaction at increasingly low p_{CO}. This is presented in Figs. 18–20 [25] (the rate is measured by the work function): from a "normal" steady state (i.e. a fixed point in the phase-space) a simple oscillating behaviour first sets in (a limit cycle), followed by period doublings (double- and fourfolded cycles) and finally by transition to aperiodic (chaotic) behaviour (a "strange" attractor).

For the Pt(1 0 0) surface neither heat effects (as usual for single-crystal experiments) nor coupling through the gas phase play a significant role in the synchronisation of the different parts. Instead, local differences in coverage initiate surface diffusion, which couples with the ongoing reaction originating a chemical wave, i.e. a steep concentration gradient travelling with constant velocity across the surface. Spatiotemporal pattern formation may thus arise.

As stated above, in the case of Pt(1 1 0) at high temperature no phase differences between different parts of the surface are to be expected. However, depending on the kind of feedback that exists between the surface reactions and the gas phase, global cou-

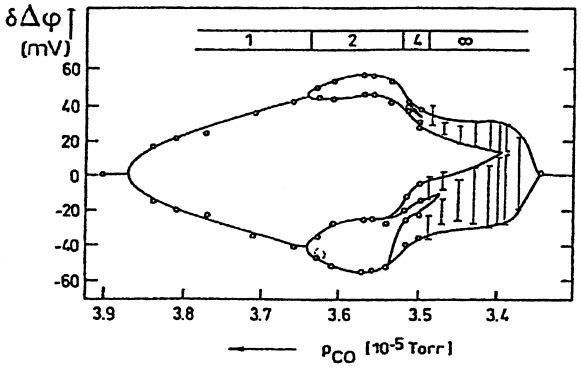

Fig. 19. Three dimensional attractors for the system in Fig. 18 (from Ref. [24]).

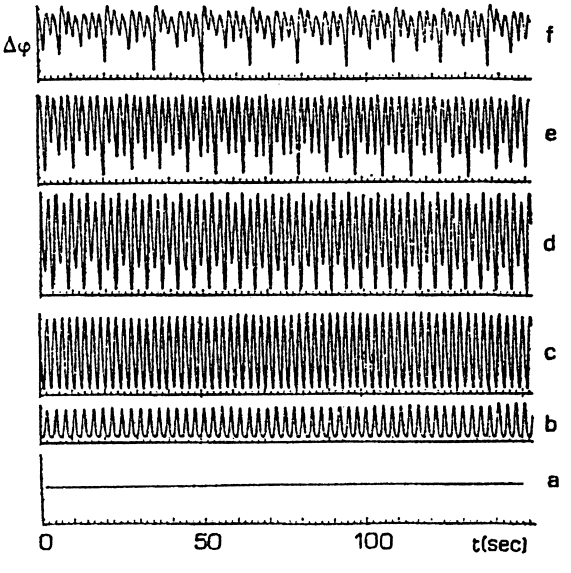

Fig. 18. Behaviour of the CO/O_2-Pt(1 1 0) system as p_{CO} is decreased. Transition from steady state (a) to: harmonic oscillation of low (b) and high amplitude (c), first period (d) and second period doubling (e), aperiodic behaviour (f) (from Ref. [24]).

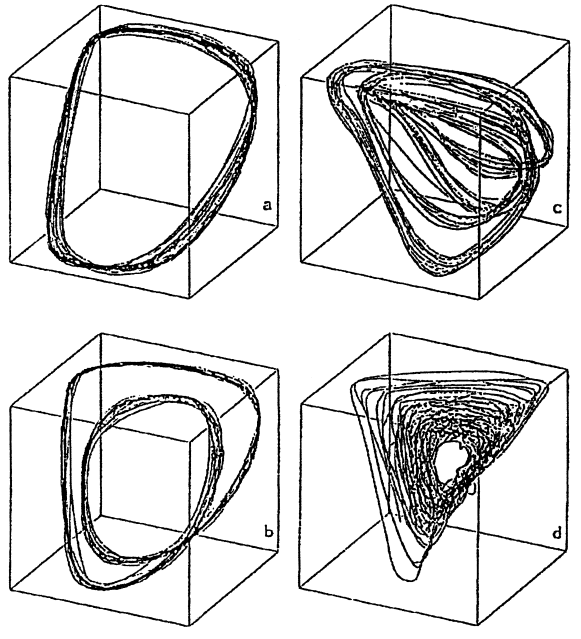

Fig. 20. Bifurcation diagram for the system of Fig. 18 (from Ref. [24]).

pling may stabilise or destabilise the homogeneously oscillating rate and symmetry breaking, i.e. pattern formation, is induced [20]. Such a synchronising influence of gas-phase coupling is revealed in the Pt(1 1 0)/CO+O_2 system at high temperature (>500 K) by the occurrence of standing waves [26]. Apart from such self-sustained spatiotemporal behaviour, pattern formation can be observed in the range of parameters (p_{O_2}, p_{CO}, T) where the system is bistable or excitable [27]. In the former case, the growth of reaction–diffusion elliptical fronts can occur (the elliptical shape is related to the anisotropy of the diffusion coefficient of adsorbed CO on the surface); in the latter, a variety of spiral waves, often pinned to surface defects, can be observed.

Stationary concentration patterns (Turing structures) can be expected in a reaction–diffusion system (cf. Section 1) one condition for their occurrence being the great difference between the diffusion rates of the reacting species. Such a condition is fulfilled on surfaces and Turing structures are actually observed in the CO+O_2 reaction on Pt(1 1 0), where the initially flat surface undergoes faceting (i.e. a periodic array of steps and terraces is formed) under the influence of the catalytic reaction.

Spatiotemporal patterns in macroscopic systems under atmospheric pressure, such as packed bed reactors, have been recently reviewed [28,29]. Due to experimental difficulties and nonuniformity of the system properties (such as catalyst loading and transport coefficients) the identification of patterns in heterogeneous reactors is still ambiguous in many cases. Such patterns should be common to many catalytic oxidation reactions and their identification is hence important for design and operation procedures in the field of pollution-abatement processes and alternate fuel production. A classification of patterns in reactors of increasing degrees of complexity (wires or ribbons, mixed and fixed-bed reactors) can be found in [29]. Such systems are quite complex, as different levels of organisation exist in heterogeneous reactors (the catalytic site, the crystallite, the pore, the pellet, the reactor), and the large-scale communication assuring the appearance of the patterns can be poor (adsorbates may diffuse and transmit information only on a continuous surface, gas-phase species diffuse only in the pore, pellet and interpellet communication is limited to heat conduction). The fast and long-range autocatalytic variable is temperature, which interacts with slow and localised changes in catalytic activity; hence, thermal effects provide the positive feedback as well as long range communication and thermal patterns may appear due to the external control or the global interaction between the fluid phase (through which the reactants are supplied) and the reactive solid phase.

Steady-state multiplicity in fixed-bed reactors has been reported [29] for CO oxidation on CuO/Al_2O_3 and Pt/Al_2O_3, ethylene oxidation on Pt/Al_2O_3. The interaction of thermal multiplicity and reactant flow may induce a periodic sequence of upstream moving pulses. Modelling [29] shows that such a behaviour is possible in adiabatic reactors when heat is adsorbed at high temperatures and produced at low temperatures, due to a second consecutive endothermic and highly activated reaction. In isothermal reactors oscillatory behaviour emerges when the reactant to the main reaction is produced by another reaction at a constant rate that is intermediate between the consumption rates at the two branches of the main reaction. Self-sustained dynamic behaviour assuming the form of successive birth and propagation of ignition and extinction fronts can occur during CO oxidation in fixed beds. An example is presented in Fig. 21 [30]: local temperature differences originated by local differences in reaction rate may, by heat conductance, propagate wavelike across an adiabatic bed and synchronise.

While the exploitation of spatial patterns for the enhancement of catalytic activity and selectivity is not within reach in the next future, the development of models dealing with the impact of pattern formation in pollution-abatement processes seems a realistic objective for future research. An example of a practical problem in this field is the optimisation of the start-up of a cold catalytic converter [29]. A heat resistant device can be used to expedite start-up and either global heating of the whole reactor or local heating producing a travelling front can be applied. Optimal distribution of the power input in space and time would be desirable, due to the limited battery power. Hence, periodic local perturbations at the inlet or outlet producing a sustained travelling pulse could represent an optimal heating policy. It should be noted however that the formulation of a realistic model accounting for the thermal effects, the temperature

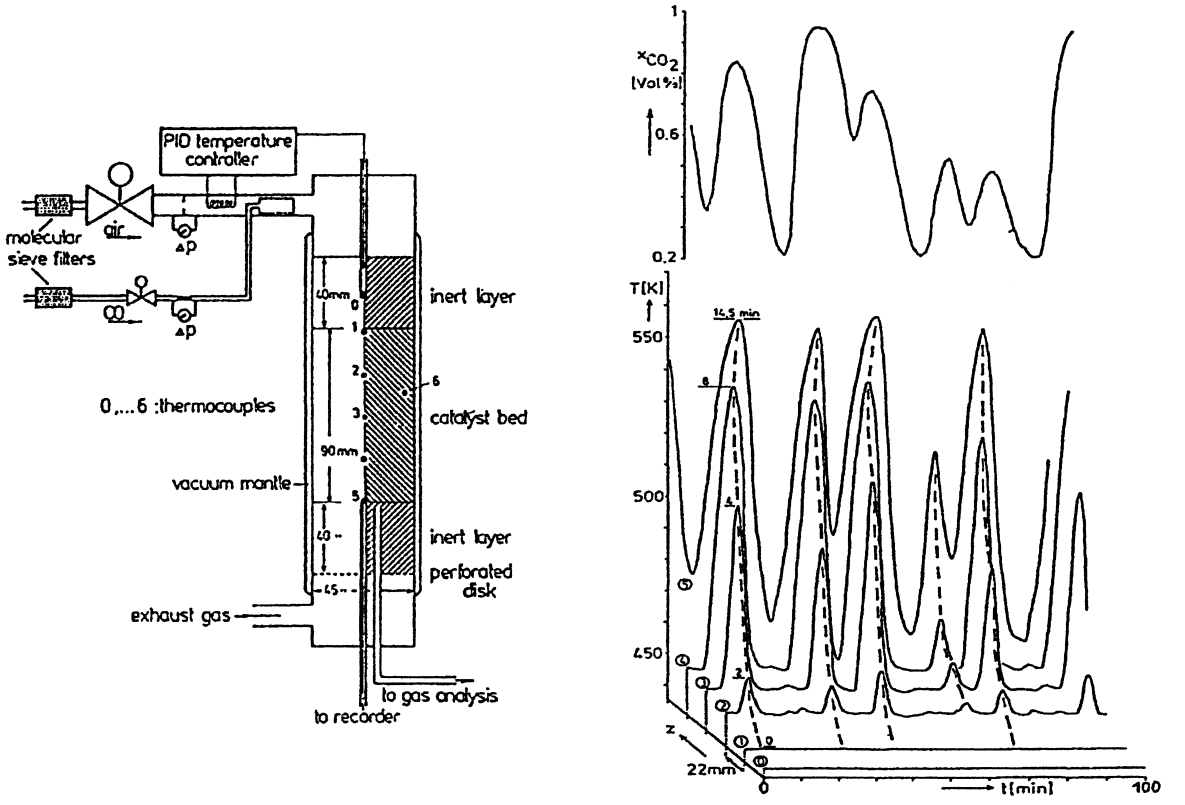

Fig. 21. Experimental device (left), temperature profiles (right below) and CO_2 concentration (right above) in the effluent for an adiabatic reactor during the catalytic CO oxidation on Pt/Al_2O_3 pellets (from Ref. [24]).

and concentration gradients between the phases, the nonlinear kinetics of surface reactions is not an easy task.

References

[1] P. Glansdorff, I. Prigogine, Thermodynamic Theory of Structure, Stability and Fluctuations, Wiley, New York, 1971.
[2] O. Bilous, N.R. Amundson, AIChE J. 1 (1995) 513.
[3] O. Bilous, N.R. Amundson, AIChE J. 2 (1956) 117.
[4] H.S. Fogler, Elements of Chemical Reaction Engineering, Prentice-Hall, Englewood Cliffs, NJ, 1986.
[5] R. Aris, Elementary Chemical Reactor Analysis, Prentice-Hall, Englewood Cliffs, NJ, 1969.
[6] R.M. Noyes, Ber. Bunsenges. Phys. Chem. 89 (1985) 620.
[7] G. Nicolis, I. Prigogine, Self Organisation in Nonequilibrium Systems, Wiley, New York, 1977.
[8] A.J. Lotka, J. Phys. Chem. 14 (1910) 271.
[9] A.J. Lotka, J. Am. Chem. Soc. 42 (1920) 1595.
[10] V. Volterra, Leçon sur la Theorie de la Lutte pour la Vie, Gauthier-Villars, Paris, 1931.
[11] A.M. Zhabotinsky, Russ. J. Phys. Chem. 42 (1968) 1649.
[12] R.J. Field, M. Burger (Eds.), Oscillations and Travelling Waves in Chemical Systems, Wiley, New York, 1985.
[13] R.M. Noyes, J. Am. Chem. Soc. 102 (1980) 4649.
[14] L. Györgyi, T. Turàny, R.J. Field, J. Phys. Chem. 94 (1990) 7162.
[15] R.J. Field, R.M. Noyes, J. Chem. Phys. 60 (1974) 1877.
[16] R.J. Field, F.W. Schneider, J. Chem. Edu. 66 (1989) 195.
[17] J.A. Pojman, R. Craven, D.C. Leard, J. Chem. Edu. 71 (1994) 84.
[18] G.J. Kasperek, T.C. Bruice, Inorg. Chem. 10 (1971) 382.
[19] B. Hess, A. Boiteux, Ber. Bunsenges. Phys. Chem. 84 (1980) 346.
[20] G. Ertl, Adv. Catal. 37 (1990) 213.
[21] F. Schüth, B.E. Henry, L.D. Schmidt, Adv. Catal. 39 (1993) 51.
[22] R. Imbihil, G. Ertl, Chem. Rev. 95 (1995) 697.
[23] M. Eiswirth, P. Möller, K. Wetzl, R. Imbihil, G. Hertl, J. Chem. Phys. 90 (1989) 510.
[24] E. Wicke, P. Kummann, W. Keil, J. Schiefler, Ber. Bunsenges. Phys. Chem. 84 (1980) 315.

[25] M. Eiswirth, K. Krisher, G. Ertl, Surf. Sci. 202 (1988) 565.
[26] S. Jacubith, H.H. Rotermund, W. Engel, A. Von Oertzen, G. Ertl, Phys. Rev. Lett. 65 (1990) 3013.
[27] S. Nettesheim, A. von Oertzen, H.H. Rotermund, G. Ertl, J. Chem. Phys. 98 (1993) 9977.
[28] M.M. Slin'ko, N.I. Jaeger, Oscillating Heterogeneous Catalytic Systems, Studies in Surface Science and Catalysis, vol. 86, Elsevier, Amsterdam, 1994.
[29] M. Sheintuch, S. Shvartsman, AIChE J. 42 (1996) 1041.
[30] H.U. Onken, E. Wicke, Ber. Bunsenges. Phys. Chem. 90 (1986) 976.